AGU PUBLICATIONS

Geophysical Research Letters

RESEARCH LETTER
10.1002/2016GL069987

Key Points:
- A local index of intraseasonal variability in the Maritime Continent is developed based on rain rates over the land and sea
- Rain rates over the land increase ahead of the main envelope of convection and decrease with the arrival of the convective envelope
- The method identifies both unambiguous MJO events and equatorial Rossby and Kelvin wave disturbances

Correspondence to:
C. L. Vincent,
claire.vincent@unimelb.edu.au

Citation:
Vincent, C. L., T. P. Lane, and M. C. Wheeler (2016), A local index of Maritime Continent intraseasonal variability based on rain rates over the land and sea, *Geophys. Res. Lett.*, *43*, 9306–9314, doi:10.1002/2016GL069987.

Received 14 JUN 2016
Accepted 19 AUG 2016
Accepted article online 23 AUG 2016
Published online 10 SEP 2016

A local index of Maritime Continent intraseasonal variability based on rain rates over the land and sea

C. L. Vincent[1,2], T. P. Lane[1,2], and M. C. Wheeler[3]

[1]School of Earth Sciences, The University of Melbourne, Melbourne, Victoria, Australia, [2]ARC Centre of Excellence for Climate System Science, [3]Bureau of Meteorology, Melbourne, Victoria, Australia

Abstract A local index for describing intraseasonal variability over the Maritime Continent is developed. The index is based on the ratio of area-averaged rain rate over the land to that over the sea. It takes advantage of the fact that the main convective envelope of intraseasonal variability events tends to modulate the diurnal precipitation cycle over the land over the entire Maritime Continent. Lagged analysis is used to create composite intraseasonal variability events, where "day 0" is chosen according to when the normalized rain rate over the sea becomes greater than that over the land. The index identifies intraseasonal variability events associated with the Madden Julian Oscillation as well as equatorial Kelvin waves and westward propagating equatorial Rossby waves. The results suggest a similar local impact of all such events in suppressing the rain rate over land relative to that over the sea when the main convective envelope approaches.

1. Introduction

Intraseasonal variability plays a dominant role in modulating weather and climate in the Maritime Continent (MC). One important contributor to intraseasonal variability is the Madden Julian Oscillation (MJO), which is associated with a large envelope of cloudiness and convection that propagates from the Indian to Pacific oceans with a period of about 30–90 days. The MJO was originally detected through spectral and cross-spectral analysis of zonal wind at 850 and 150 hPa and surface pressure, with peaks in the variance and coherence spectra at periods of 41–53 days [*Madden and Julian*, 1971]. With the advent of satellite observations of fields such as outgoing longwave radiation (OLR), space-time spectral analysis has become a standard tool for identifying equatorial waves. For example, *Wheeler and Kiladis* [1999] performed space-time spectral analysis of satellite-derived OLR and identified the MJO with a period of around 40 days, as well as Kelvin and other equatorial waves. They demonstrated that space-time spectral filtering could be used to isolate the MJO, Kelvin waves, equatorial Rossby waves, and mixed Rossby gravity waves. Another widely used method of identifying the MJO is through empirical orthogonal function (EOF) analysis of wind and OLR. *Wheeler and Hendon* [2004] pioneered development of a real-time MJO index based on coefficients of the first two EOFs of OLR and zonal wind at 200 hPa and 850 hPa, latitudinally averaged between 15°S and 15°N (hereafter the WH04 index). The leading two EOFs form a pair that allow for the MJO to be represented in a two-dimensional phase space with a defined phase and amplitude each day. They divided the phase into eight segments, which have been interpreted as a set of eight "MJO categories" that have been used for numerous conditional averaging and MJO propagation studies [e.g., *Oh et al.*, 2013; *Peatman et al.*, 2014; *Vincent and Lane*, 2016]. *Kiladis et al.* [2014] developed an analogous index based only on filtered OLR (the OMI index) and showed similar average circulation patterns to those from the WH04 index, but substantial differences when considering individual events.

While the MJO has been shown to explain many aspects of variability in rainfall and convection in the MC, there are other influences including Kelvin and Rossby wave disturbances that contribute to intraseasonal variability. Furthermore, there is a lack of consensus on what should be classified as MJO events, especially in the MC where the MJO signal can be strongly modified. For example, during the "Dynamics of the MJO" (DYNAMO) field campaign [*Yoneyama et al.*, 2013], five major eastward propagating intraseasonal variability events were observed between October 2011 and March 2012. Three of these events are identified unambiguously as MJO events by the WH04 index, but two (in December 2011 and January 2012) are not. Whether these remaining two events should be considered as MJO events has been debated [e.g., *Yoneyama et al.*, 2013; *Ling et al.*, 2014; *Yokoi and Sobel*, 2015].

The ambiguity in classifying eastward propagating disturbances as MJO events is compounded by the fact that some MJO events initiating in the Indian Ocean weaken or dissipate altogether as they reach the MC [e.g., *Oh et al.*, 2013; *Feng et al.*, 2015]. The eastward passage of the MJO is interrupted by the complex archipelago of the MC, and its propagation and evolution through the region are controlled by interaction of global-scale variability with mesoscale dynamics. Although a precise definition of MJO events over the MC is problematic, the practical implications of large eastward or westward propagating MJO or non-MJO convective envelopes are linked by some common threads. As argued by *Peatman et al.* [2014] and *Birch et al.* [2016], clear skies and a moist environment prior to the arrival of the large-scale convective envelope promote favorable conditions for the diurnal precipitation cycle and heavy rainfall over the land, while the main convective envelope suppresses solar radiation at the surface and dampens the diurnal cycle over the land. Indeed, *Peatman et al.* [2014] suggests that in areas with a strong diurnal cycle, most of the MJO-scale variation in rain rate in the MC is due to variations in the amplitude of the diurnal cycle.

We propose an intraseasonal variability index over the MC based on the physical processes leading to differential evolution of rain rates over the land and sea — namely, the normalized ratio of rain rate over the land to that over the sea. Many events identified by the index correspond to MJO events identified by the WH04 index. In contrast to previously published MJO indices [*Wheeler and Hendon*, 2004; *Kiladis et al.*, 2014], our index uses local information that implicitly includes the mesoscale dynamics of the MC. It therefore takes into account any modulation of local propagation speed relative to the large-scale circulation indices and includes MJO-like disturbances that may be only weakly present in large-scale circulation-based indices but nevertheless show eastward propagation, such as the December 2011 and January 2012 DYNAMO events. Furthermore, our index shows that similar relationships between rain rates over the land and sea exist for identified Kelvin and equatorial Rossby wave events. The rain rate index is therefore useful as a local compositing tool over the MC, although may not be useful for identifying intraseasonal variability over the Indian or Pacific Oceans.

Our index also differs from previously proposed event-based indices derived from a precipitation maximum or OLR minimum because it is designed specifically for the MC where strong convection over the land in the lead-up to active MJO periods would confound any attempt to use area-averaged rainfall alone. Existing indices based on precipitation or OLR are excellently suited to identifying MJO initiation over the Indian Ocean where topographic effects need not be considered. Several event-based MJO indices have been proposed [e.g., *Ling et al.*, 2013; *Marshall et al.*, 2008; *Feng et al.*, 2015; *Benedict and Randall*, 2007], but these methods all involve searching for "day 0" in OLR or precipitation data that have already been filtered for MJO scales, while our method involves no a priori assumptions about spatial or temporal scales.

In this paper, we first describe the statistical properties of time series of area-averaged rain rate over the sea and land that are used to derive the local intraseasonal variability index, then present the index itself and its relationship to the WH04 index (section 3). In section 4, events identified by the rain rate and WH04 indices are compared with MJO events, Kelvin waves, and equatorial Rossby waves evident in filtered OLR anomalies. Finally, in section 5 composite precipitation and OLR anomalies for intraseasonal events identified with the new index are presented.

2. Data

The local intraseasonal variability index is derived using 17 years of austral summer (1 December–28 February) satellite precipitation estimates over the MC from the Tropical Rainfall Measuring Mission (TRMM) 3B42 V7 product [*Huffman et al.*, 2007]. The data are on a 0.25° × 0.25° latitude/longitude grid and are available at 3-hourly intervals centered about 0000–2100 UTC. The region used for the analysis is shown in Figure 1, together with the average austral summer (December–February) rainfall for the 17 year period. The highest average rain rates are over the land, in particular, over the steepest topography, and within several hundred kilometers of the coast. Similar analyses performed over smaller regions (not shown) showed that the rain rate index is relatively insensitive to choice of area. TRMM products have been shown to underestimate rainfall over high topography [e.g., *Stampoulis and Anagnostou*, 2012] and to have a systematic lag in the timing of the diurnal precipitation peak [e.g., *Rauniyar and Walsh*, 2013], but for the purposes of this analysis these systematic errors are less important than the relative evolution of daily rain rate with the passage of intraseasonal variability events. Gridded daily OLR anomalies from NOAA [*Liebmann and Smith*, 1996] were also used to identify intraseasonal variability events using space-time filtering and to create composite OLR anomaly intraseasonal variability events.

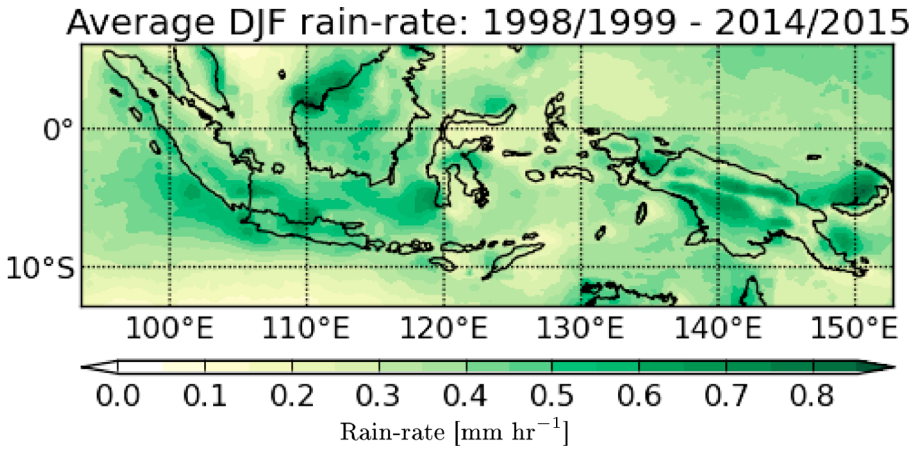

Figure 1. The 17 year average austral summer precipitation from TRMM. The map indicates the area considered the "Maritime Continent" in this study.

3. A Local Intraseasonal Variability Index Over the Maritime Continent

Time series of area-averaged rain rate over the land (rr_L) and sea (rr_S) in the MC were calculated by applying the TRMM land-sea mask and averaging to daily values. rr_{ind} is defined by the ratio of rr_L to rr_S, normalized by the ratio of their seasonal averages for each DJF period:

$$rr_{\text{ind}} = \frac{rr_L}{rr_S}\frac{\overline{rr_S}}{\overline{rr_L}}, \tag{1}$$

where $\overline{rr_L}$ and $\overline{rr_S}$ are the seasonal average rain rates over the land and sea, respectively.

Normalization means that when rr_{ind} is greater than 1, the rain rate over the land relative to its seasonal average is greater than the rain rate over the sea relative to its seasonal average, and when rr_{ind} is less than 1, the opposite is true. Finally, a 1-2-1 temporal smoother is applied to rr_{ind}.

To test the hypothesis that rr_{ind} becomes less than unity as the MJO passes over the MC, it was conditionally averaged according to the eight WH04 MJO phases for the period 1998–2014. The average austral summer rr_{ind} as a function of WH04 index is shown in Figure 2. As hypothesized, rr_{ind} decreases to less than unity for WH04 categories 4, 5, and 6, which are phases normally considered as MJO-active over the MC.

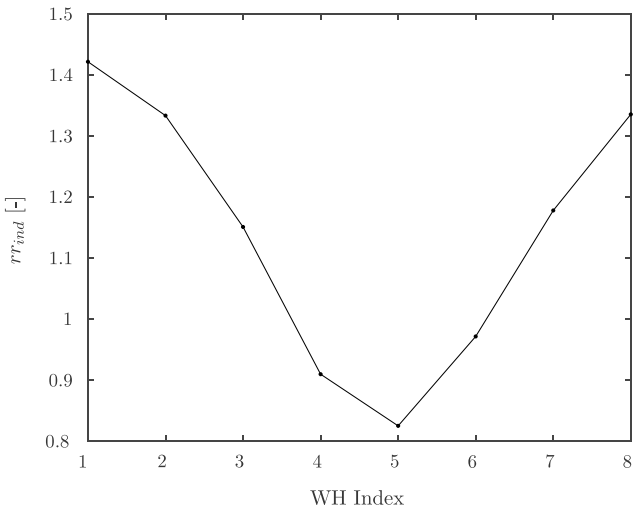

Figure 2. Average value of rr_{ind} for MJO phase as classified by the WH04 index.

4. Definition of Intraseasonal Events Using rr_{ind}

We define day 0 of an intraseasonal event as a day where rr_{ind} changes from being greater than to less than 1. To avoid including small fluctuations in rr_{ind}, for any day n to be considered as a day 0, it must satisfy the following criteria:

$$\frac{1}{3}(rr_{ind}[n-3] + rr_{ind}[n-2] + rr_{ind}[n-1]) > 1 \text{ and} \tag{2}$$

$$\frac{1}{3}(rr_{ind}[n] + rr_{ind}[n+1] + rr_{ind}[n+2]) < 1. \tag{3}$$

To avoid contamination by a single large spike, we also ensure that at least 5 out of 8 days prior to day n are greater than 1, and at least 5 out of 8 days after day n are less than 1. Finally, events occurring less than 10 days after the previous event are rejected, and the difference between the maximum value of rr_{ind} in the 10 days before day n and the minimum value of rr_{ind} in the 10 days after day n should be greater than 0.7. This final criterion measures event amplitude and was chosen to discard the weakest 10% of events.

A set of MJO events were also defined using the WH04 index. For day n to be considered as a day 0, the following criteria must be satisfied:

$$\frac{1}{3}(wh_{ind}[n-3] + wh_{ind}[n-2] + wh_{ind}[n-1]) < 4 \text{ and} \tag{4}$$

$$\frac{1}{3}(wh_{ind}[n] + wh_{ind}[n+1] + wh_{ind}[n+2]) >= 4, \tag{5}$$

where wh_{ind} is the WH04 phase. Here a phase of 4 is used because it is normally used to define active MJO conditions in the MC. Events occurring less than 10 days after the previous event are rejected. Furthermore, the average amplitude of the WH04 index should be greater than 0.8 for 3 days before and after day n, where the threshold was chosen to discard the weakest 10% of events.

The average evolution of rr_S, rr_L, and rr_{ind} for all events defined by day 0 from rr_{ind} and WH04, respectively, are shown in Figure 3. rr_{ind} based on the day 0 definitions from rr_{ind} itself has a sharper gradient as it transitions from values above 1 to values below 1 than when the day 0 definitions from the WH04 index are used, indicating the more local definition and the shorter time scales involved in rr_{ind}.

The properties of rr_{ind} are further demonstrated in Figure 4, where Hovmöller diagrams of TRMM estimates over the MC are shown together with OLR anomalies for the full range of longitudes. The OLR data are averaged between latitudes of 10°S and 5°N. While intraseasonal events can be qualitatively identified from the Hovmöller diagrams, rr_{ind} has the advantage that it does not involve a priori assumptions about the temporal or spatial scales of the events, and implicitly handles the combined local mesoscale impact of interacting modes of variability. Four selected austral summer seasons are shown. For the TRMM precipitation, day 0 of events as identified by the WH04 index and rr_{ind} are shown as dashed and solid black lines, respectively. For the OLR anomalies, filtered MJO, Kelvin waves and equatorial Rossby wave signals are indicated, since inspection of space-time spectra (not shown) and results such as those in *Wheeler and Kiladis* [1999] and *Wheeler and Weickmann* [2001] suggest that these are the major sources of intraseasonal variability. The filtering follows the methodology of *Wheeler and Kiladis* [1999], with retained signals for Kelvin and equatorial Rossby waves following dispersion curves for equivalent depths of 8–90 m. The MJO is treated as a rectangular box in frequency-wave number space including the first five zonal wave numbers and temporal scales of 30–90 days.

During the 2000–2001 austral summer (Figures 4a and 4e), an unambiguous MJO event reaching the MC around 1 February is identified by both the WH04 index and rr_{ind}. However, there is also an event identified only by rr_{ind} in early January, which coincides with both a Kelvin wave disturbance and a westward moving equatorial Rossby wave (Figure 4e). Indeed, the formulation rr_{ind} does not constrain it to eastward propagating events, and the TRMM anomalies (Figure 4a) also indicate westward moving disturbances during this time. In the 2003–2004 season (Figures 4b and 4f), there are two unambiguous MJO events that are detected by both rr_{ind} and the WH04 index with a difference of only 1–2 days. In all strong, unambiguous MJO cases, agreement between the two indices is excellent.

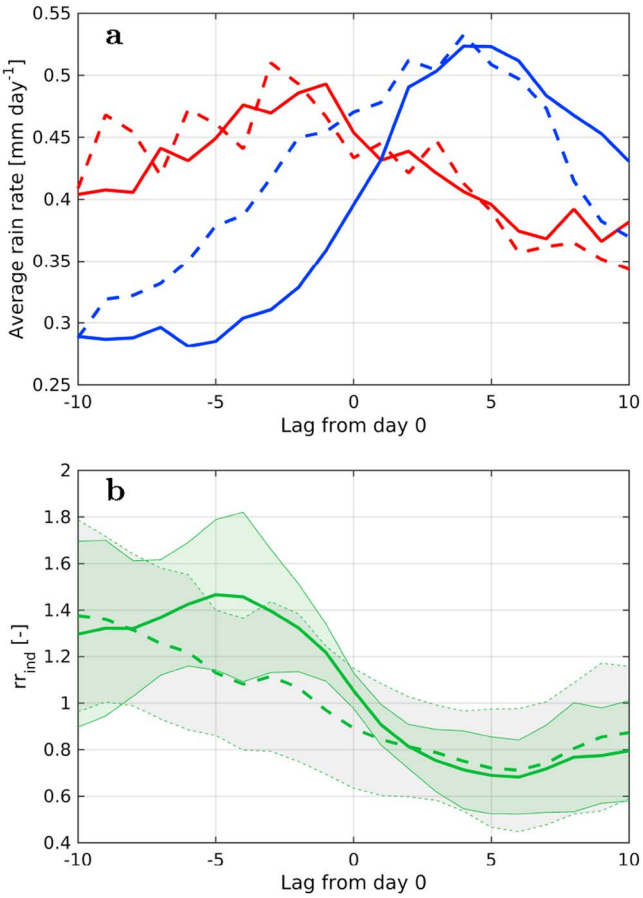

Figure 3. (a) Average rain rates over land (rr_L, red) and sea (rr_S, blue) as a function of lag, with day 0 defined using rr_{ind} (solid) and the WH04 index (dashed). (b) Average rr_{ind} for day 0 defined by rr_{ind} (solid thick line with one standard deviation from the mean in green shading and thin solid lines) and the WH04 index (dashed with one standard deviation from the mean in grey shading and thin dashed lines). Averages include 25 events identified by the WH04 index and 37 events identified by rr_{ind}.

During the 2004–2005 austral summer (Figures 4c and 4g), the filtered OLR reveals a complex interaction of weak MJO events, Kelvin waves, and westward moving equatorial Rossby waves. One clear MJO event in late December is identified by the WH04 index and rr_{ind} with a difference of several days, but there are Kelvin waves and strong equatorial Rossby wave disturbances intersecting the MJO signal that could have triggered rr_{ind} to reach its threshold ahead of the MJO event. A band of eastward propagating precipitation appears to correspond to a double Kelvin wave feature around 1 February.

The 2011–2012 austral summer (Figures 4d and 4h) is of particular interest because it occurred during the DYNAMO field campaign [*Yoneyama et al.*, 2013]. An eastward propagating MJO-like disturbance in December is not obvious in the MJO filtering conducted here, although it is identified if temporal filtering is extended to 20–90 days (not shown). This event is also not identified by the WH04 index, but whether this event should be considered an MJO has been debated. For example, *Yoneyama et al.* [2013] argued that although the event is weakly identified in OLR data, it is not identified by the WH04 index and can be considered a "hiccup" of the previous event. *Ling et al.* [2014] noticed that while the event was obvious in TRMM data, it was not identified by the WH04 index. *Yokoi and Sobel* [2015] considered both the December 2011 and the subsequent January 2012 events as MJO events, based on TRMM data and phase relations between moisture, precipitation, and wind. Our analysis indicates that there are both Kelvin and westward moving equatorial Rossby waves coinciding with the weak MJO-like signals. In particular, the westward moving signals are evident in the TRMM anomalies and may have triggered rr_{ind} to identify these events.

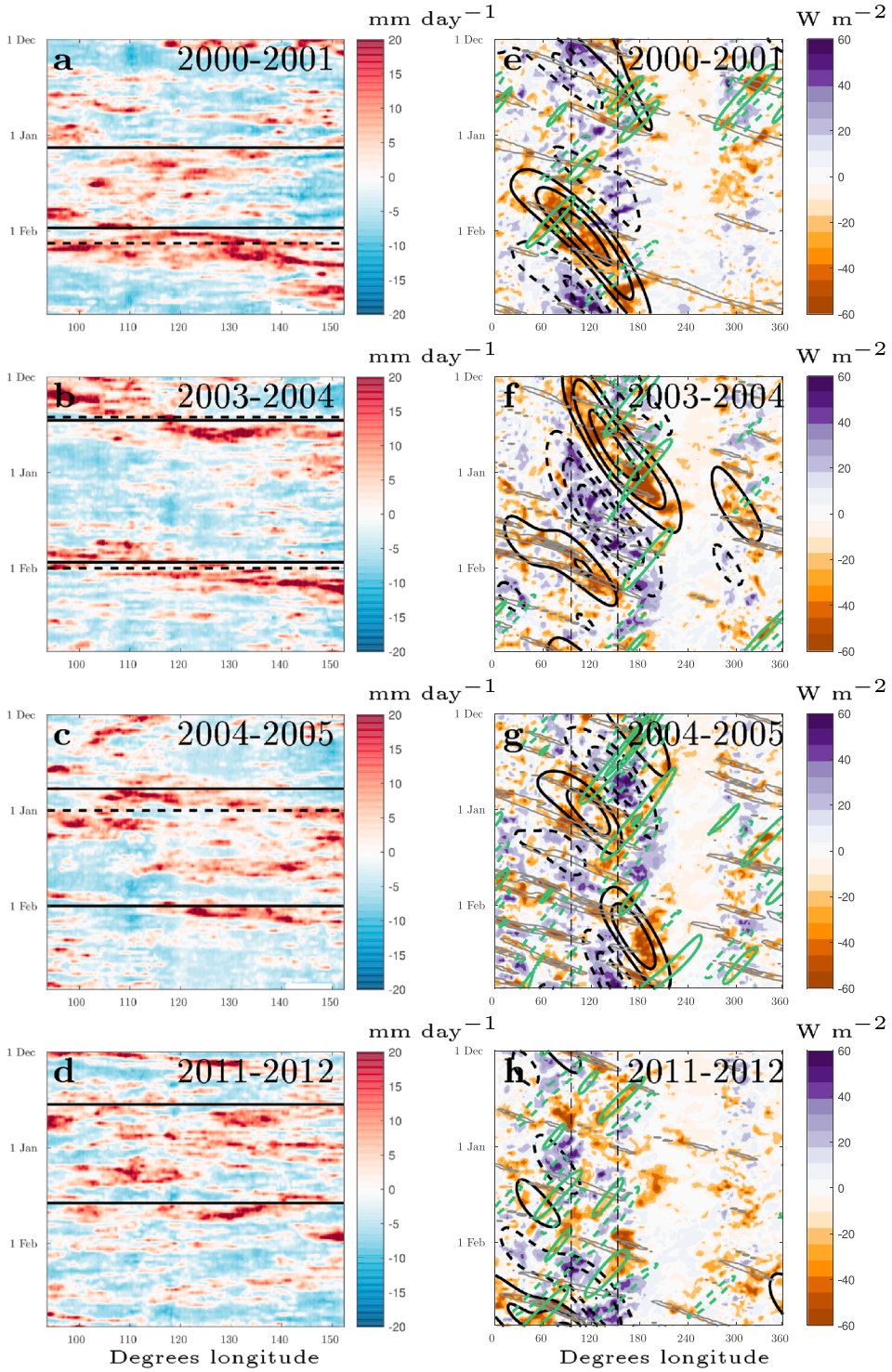

Figure 4. (a–d) Hovmöller diagrams of TRMM precipitation anomaly estimates over the MC for the austral summer seasons 2000–2001 (Figure 4a), 2003–2004 (Figure 4b), 2004–2005 (Figure 4c), and 2011–2012 (Figure 4d). MJO Events identified by the WH04 index and rr_{ind} are shown as dashed and solid black lines, respectively. (e–h) Hovmöller diagrams of OLR anomaly, averaged between 10°S and 5°N for the austral summer seasons 2000–2001 (Figure 4e), 2003–2004 (Figure 4f), 2004–2005 (Figure 4g), and 2011–2012 (Figure 4h). The first three annual harmonics are removed from the data, and it is detrended. Shading: unfiltered data. Black, green, and grey line contours: OLR filtered in space-time for the MJO, equatorial Rossby waves, and Kelvin waves, respectively, with contour intervals of 10 W m^{-2}. Dashed contours show positive anomalies, and solid contours show negative anomalies, except for Kelvin waves where only negative anomalies are shown for clarity. Thin dashed vertical lines indicate the position of the MC.

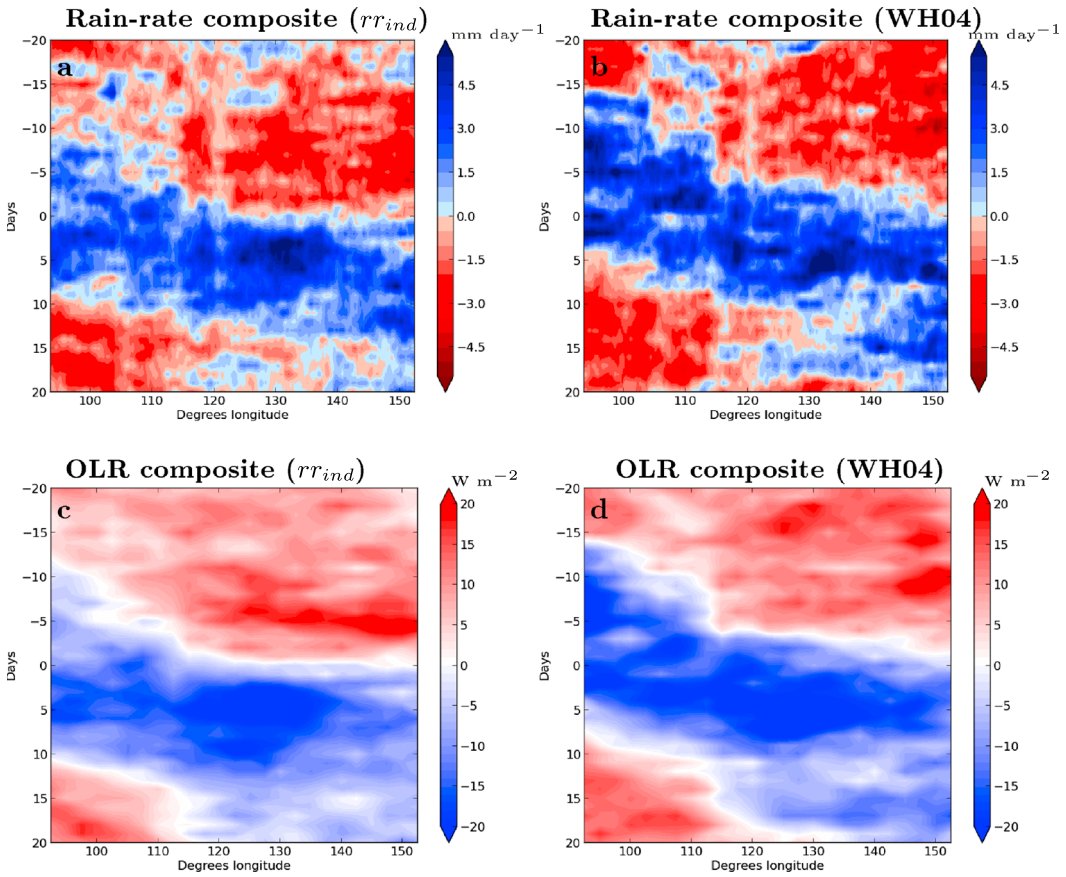

Figure 5. (a and b) Composite austral summer events from TRMM, using day 0 defined by rr_{ind} (Figure 5a) and the WH04 index (Figure 5b). (c and d) Equivalent plots for OLR.

5. Composite Intraseasonal Variability Events

The rr_{ind} and WH04 indices were each used to define a 17 year composite austral summer intraseasonal variability event (Figure 5) for precipitation (a and b) and OLR (c and d). Despite the difference in the definition of events, the composites show remarkable similarity. The anomalies are weaker in the rr_{ind} composite because this method includes weaker MJO-like events, Kelvin waves, and even westward propagating equatorial Rossby waves, but the overall structure of the composites is nearly identical. The composites from both methods suggest that the MJO speeds up as it reaches the MC. Furthermore, the trailing and leading edges of the precipitation and OLR anomalies pause for 3–5 days at around 115°E, corresponding with the position of Borneo.

To explore the role of the major MC islands in this uneven progression of the precipitation anomaly, the analysis in Figures 5a and 5b was repeated for land and water points, respectively (Figure 6). There was at least one land point at every longitude, but the number of points included in the average varies with longitude, leading to the patchy contours. However, the role of the topography is clear. Heavy rain starts over the longitudinal extent of Borneo around 5–6 days ahead of the precipitation over the water, which follows a more gradual progression, and there is a similar pattern around the longitudes corresponding to Sumatra and the Malay Peninsula. This may be due to the static forcing from steep topography playing a greater role than the gradually moistening environment in controlling the onset of heavy precipitation, consistent with the arguments of *Bergemann and Jakob* [2016] who showed that near the coast, precipitation could be initiated in a drier environment than over the open ocean.

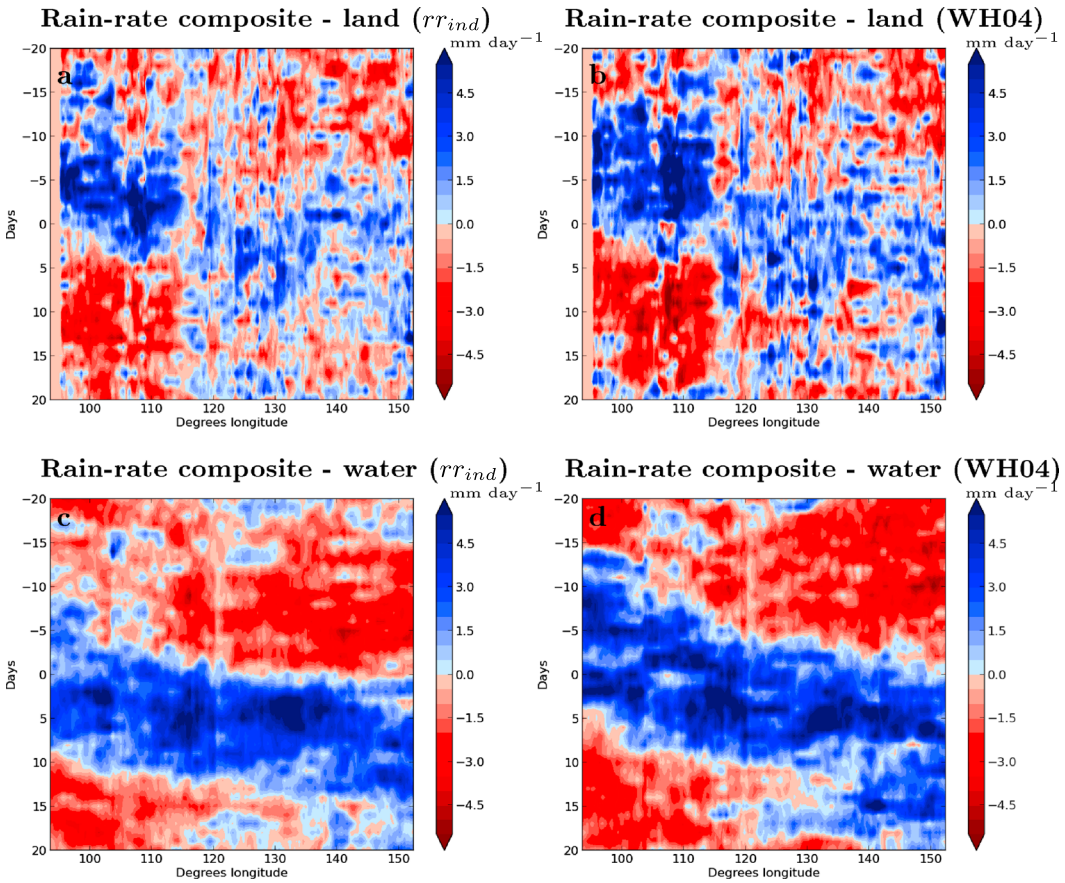

Figure 6. (a and b) Composite austral summer events from TRMM land points, using day 0 defined by rr_{ind} (Figure 6a) and the WH04 index (Figure 6b). (c and d) Equivalent plots for TRMM water points.

6. Discussion and Conclusions

We developed a new local intraseasonal variability index for the MC based on the ratio of area-averaged rain rates over the sea and land. The index was used to define a set of composite intraseasonal variability events. The events included MJO events, Kelvin waves, and westward propagating equatorial Rossby waves. For the MJO events, there was excellent agreement between the local index and the WH04 index. Our analysis suggests that as an intraseasonal variability event propagates either eastward or westward through the MC, the relative evolution of rain rates over the land and sea may be relatively invariant to the type of disturbance.

Most of the intraseasonal variability events identified by rr_{ind} were found to occur in the presence of MJO events or equatorial Rossby or Kelvin waves. However, extricating the relative contribution of these modes of variability over the MC, where steep topography and complex coastlines introduce a mesoscale response to the large-scale variability is problematic. For example, the December 2011 and January 2012 MJO-like events during DYNAMO include both eastward and westward aspects to the propagating disturbances. We have not considered the possible different performance of TRMM over land and sea, in particular, over steep topography, which could influence the results, but this is not expected to influence the qualitative application of the index.

The analysis herein shows that the signatures of all the intraseasonal variability events on the evolution of the relative rain rates over land and sea are similar. The enhanced daily average rain rate over the land prior to the onset of an intraseasonal variability event is likely to correspond to an increase in the amplitude of the diurnal precipitation cycle as a result of clear skies and a moistening environment. Conversely, suppressed rain rate over the land as the main convective envelope approaches is likely linked to decreased radiative forcing and therefore a smaller diurnal precipitation cycle. These factors have been discussed by *Peatman et al.* [2014], *Vincent and Lane* [2016], and *Birch et al.* [2016] and others in relation to the MJO. In particular, there has

been recent focus on whether a realistic diurnal precipitation cycle is important for accurate MJO propagation through the MC in regional and climate models [e.g., *Peatman et al.*, 2015; *Birch et al.*, 2016]. Our results suggest that the interplay between the diurnal precipitation cycle and onset of the envelope of intraseasonal positive precipitation anomalies may reflect a more general relationship.

Acknowledgments
This work was funded by the Australian Research Council's Centre of Excellence for Climate System Science (CE110001028). Analysis was partly undertaken on the National Computational Infrastructure (NCI), which is supported by the Australian Government. Helpful discussions with Eric Maloney (Colorado State University) and assistance from Paola Petrelli (NCI) and Malcolm King (The University of Melbourne) are gratefully acknowledged. Thanks to Charmaine Franklin and Surendra Rauniyar (Australian Bureau of Meteorology) and two anonymous reviewers for helpful comments on the manuscript. Interpolated OLR data were downloaded from NOAA/OAR/ESRL PSD (http://www.esrl.noaa.gov/psd/). TRMM 3-hourly precipitation estimates were downloaded from the Goddard Earth Sciences Data and Information Services Center (ftp://disc2.nascom.nasa.gov/data/s4pa/TRMM_L3/TRMM_3B42/).

References

Benedict, J. J., and D. A. Randall (2007), Observed characteristics of the MJO relative to maximum rainfall, *J. Atmos. Sci.*, *64*(7), 2332–2354, doi:10.1175/JAS3968.1.

Bergemann, M., and C. Jakob (2016), How important is tropospheric humidity for coastal rainfall in the tropics?, *Geophys. Res. Lett.*, *43*(11), 5860–5868, doi:10.1002/2016GL069255.

Birch, C., S. Webster, S. C. Peatman, D. Parker, A. Matthews, Y. Li, and M. Hassim (2016), Scale interactions between the MJO and the western Maritime Continent, *J. Clim.*, *29*, 2471–2492.

Feng, J., T. Li, and W. Zhu (2015), Propagating and nonpropagating MJO events over Maritime Continent, *J. Clim.*, *28*(21), 8430–8449, doi:10.1175/JCLI-D-15-0085.1.

Huffman, G. J., D. T. Bolvin, E. J. Nelkin, D. B. Wolff, R. F. Adler, G. Gu, Y. Hong, K. P. Bowman, and E. F. Stocker (2007), The TRMM Multisatellite Precipitation Analysis (TMPA): Quasi-global, multiyear, combined-sensor precipitation estimates at fine scales, *J. Hydrometeorol.*, *8*, 38–55, doi:10.1175/JHM560.1.

Kiladis, G. N., J. Dias, K. H. Straub, M. C. Wheeler, S. N. Tulich, K. Kikuchi, K. M. Weickmann, and M. J. Ventrice (2014), A comparison of OLR and circulation-based indices for tracking the MJO, *Mon. Weather Rev.*, *142*, 1697–1715, doi:10.1175/MWR-D-13-00301.1.

Liebmann, B., and C. A. Smith (1996), Description of a complete (interpolated) outgoing longwave radiation dataset, *Bull. Am. Meteorol. Soc.*, *77*(6), 1275–1277.

Ling, J., C. Zhang, and P. Bechtold (2013), Large-scale distinctions between MJO and non-MJO convective initiation over the tropical Indian Ocean, *J. Atmos. Sci.*, *70*(9), 2696–2712, doi:10.1175/JAS-D-13-029.1.

Ling, J., P. Bauer, P. Bechtold, A. C. M. Beljaars, R. Forbes, F. Vitart, M. Ulate, and C. Zhang (2014), Global versus local MJO forecast skill of the ECMWF model during DYNAMO Indian Ocean experiment on intraseasonal variability in, *Mon. Weather Rev.*, *142*, 2228–2247, doi:10.1175/MWR-D-13-00292.1.

Madden, R. A., and P. R. Julian (1971), Detection of a 40–50 day oscillation in the zonal wind in the Tropical Pacific, *J. Atmos. Sci.*, *28*, 702–708, doi:10.1175/1520-0469(1971)028<0702:DOADOI>2.0.CO;2.

Marshall, A. G., O. Alves, and H. H. Hendon (2008), An enhanced moisture convergence-evaporation feedback mechanism for MJO air-sea interaction, *J. Atmos. Sci.*, *65*(3), 970–986, doi:10.1175/2007JAS2313.1.

Oh, J.-H., B.-M. Kim, K.-Y. Kim, H.-J. Song, and G.-H. Lim (2013), The impact of the diurnal cycle on the MJO over the Maritime Continent: A modeling study assimilating TRMM rain rate into global analysis, *Clim. Dyn.*, *40*, 893–911, doi:10.1007/s00382-012-1419-8.

Peatman, S. C., A. J. Matthews, and D. P. Stevens (2014), Propagation of the Madden-Julian oscillation through the Maritime Continent and scale interaction with the diurnal cycle of precipitation, *Q. J. R. Meteorol. Soc.*, *140*(680), 814–825, doi:10.1002/qj.2161.

Peatman, S. C., A. J. Matthews, and D. P. Stevens (2015), Propagation of the Madden-Julian oscillation and scale interaction with the diurnal cycle in a high-resolution GCM, *Clim. Dyn.*, *45*, 2901–2918, doi:10.1007/s00382-015-2513-5.

Rauniyar, S. P., and K. J. E. Walsh (2013), Scale interaction of the diurnal cycle of rainfall over the MC and Australia: Influence of the MJO, *J. Clim.*, *26*, 1304–1321.

Stampoulis, D., and N. Anagnostou (2012), Evaluation of global satellite rainfall products over continental Europe, *J. Hydrometeorol.*, *13*, 588–603.

Vincent, C. L., and T. P. Lane (2016), Evolution of the diurnal precipitation cycle with the passage of a Madden-Julian oscillation event through the Maritime Continent, *Mon. Weather Rev.*, *144*, 1983–2005, doi:10.1175/MWR-D-15-0326.1.

Wheeler, M., and G. N. Kiladis (1999), Convectively coupled equatorial waves: Analysis of clouds and temperature in the wavenumber–frequency domain, *J. Atmos. Sci.*, *56*, 374–399, doi:10.1175/1520-0469(1999)056<0374:CCEWAO>2.0.CO;2.

Wheeler, M., and K. M. Weickmann (2001), Real-time monitoring and prediction of modes of coherent synoptic to intraseasonal tropical variablity, *Mon. Weather Rev.*, *129*, 2677–2677.

Wheeler, M. C., and H. H. Hendon (2004), An all-season real-time multivariate MJO index: Development of an index for monitoring and prediction, *Mon. Weather Rev.*, *132*, 1917–1932.

Yokoi, S., and A. H. Sobel (2015), Intraseasonal variability and seasonal March of the moist static energy budget over the eastern Maritime Continent during CINDY2011/DYNAMO, *J. Meteorol. Soc. Jpn.*, *93A*, 81–100, doi:10.2151/jmsj.2015-041.

Yoneyama, K., C. Zhang, and C. N. Long (2013), Tracking pulses of the Madden-Julian oscillation, *Bull. Am. Meteorol. Soc.*, *94*(12), 1871–1891, doi:10.1175/BAMS-D-12-00157.1.